



Published in final edited form as:

J Comp Neurol. 2010 November 1; 518(21): 4375–4394. doi:10.1002/cne.22462.

Tuberoinfundibular Peptide of 39 Residues Modulates the Mouse Hypothalamic–Pituitary–Adrenal Axis Via Paraventricular Glutamatergic Neurons

Eugene Dimitrov and Ted Björn Usdin*

Section on Fundamental Neuroscience, National Institute of Mental Health, Bethesda, Maryland 20892

Abstract

Neurons in the subparafascicular area at the caudal border of the thalamus that contain the neuropeptide tuberoinfundibular peptide of 39 residues (TIP39) densely innervate several hypothalamic areas, including the paraventricular nucleus (PVN). These areas contain a matching distribution of TIP39's receptor, the parathyroid hormone receptor 2 (PTH2R). Frequent PTH2R coexpression with a vesicular glutamate transporter (VGlut2) suggests that TIP39 could presynaptically regulate glutamate release. By using immunohistochemistry we found CRH-ir neurons surrounded by PTH2R-ir fibers and TIP39-ir axonal projections in the PVN area of the mouse brain. Labeling hypothalamic neuroendocrine neurons by peripheral injection of fluorogold in PTH2R-lacZ knock-in mice showed that most PTH2Rs are on PVN and peri-PVN interneurons and not on neuroendocrine cells. Double fluorescent *in situ* hybridization revealed a high level of coexpression between PTH2R and VGlut2 mRNA by cells located in the PVN and nearby brain areas. Local TIP39 infusion (100 pmol) robustly increased pCREB-ir in the PVN and adjacent perinuclear zone. It also increased plasma corticosterone and decreased plasma prolactin. These effects of TIP39 on pCREB-ir, corticosterone, and prolactin were abolished by coinjection of the ionotropic glutamate receptor antagonists 6-cyano-7-nitroquinoxaline-2,3-dione (CNQX) and DL-2-amino-5-phosphonopentanoic acid (AP-5; 30 pmol each) and were absent in PTH2R knockout mice. Basal plasma corticosterone was slightly decreased in TIP39 knockout mice just before onset of their active phase. The present data indicate that the TIP39 ligand/PTH2 receptor system provides facilitatory regulation of the hypothalamic–pituitary–adrenal axis via hypothalamic glutamatergic neurons and that it may regulate other neuroendocrine systems by a similar mechanism.

Keywords

neuropeptide; presynaptic facilitation; stress; paraventricular nucleus; parathyroid hormone 2 receptor; neuroendocrine

The stress response helps the organism adapt to abrupt environmental changes. Hypothalamic–pituitary–adrenal (HPA) axis activation is its main feature (Charmandari et al., 2005). Signals generated by adverse physical and psychogenic stimuli are directed to the hypothalamic paraventricular nucleus (PVN; Herman et al., 2003; Van de Kar and Blair, 1999) by fibers containing classical neurotransmitters and/or neuropeptides (Sawchenko and Swanson, 1982; Sawchenko et al., 1985; Swanson and Sawchenko, 1983) that synapse

*CORRESPONDENCE TO: T.B. Usdin, Bldg. 35/Room 1B-215, 35 Convent Dr., MSC 3728, Bethesda, MD 20892. usdint@mail.nih.gov.

Additional Supporting Information may be found in the online version of this article.

directly with neuroendocrine cells, or influence the neuroendocrine cells indirectly via local GABAergic or glutamatergic interneurons (Boudaba et al., 1996; Cole and Sawchenko, 2002; Herman et al., 1996, 2002; Lin et al., 2003; Roland and Sawchenko, 1993). PVN neuroendocrine cells respond by releasing adrenocorticotropin (ACTH) secretagogues, corticotropin-releasing hormone (CRH) being the most powerful (Liposits, 1993; Sawchenko and Swanson, 1985). Pituitary ACTH then stimulates adrenal glucocorticosteroid secretion, which facilitates adaptive changes throughout the body (Charmandari et al., 2005). Thus, PVN output results from a fine balance between stimulatory and inhibitory signals that reach the nucleus.

Tuberoinfundibular peptide of 39 residues (TIP39) is a neuropeptide that may modulate HPA axis activity. TIP39 belongs to a polypeptide family that includes parathyroid hormone, parathyroid hormone-related peptide, CRH, vasoactive intestinal polypeptide, glucagon, and calcitonin (Brown et al., 1996; Usdin et al., 1999). TIP39 neurons in the subparafascicular area, at the caudal border of the thalamus, project to hypothalamic areas (Dobolyi et al., 2003b), which contain a matching distribution of its receptor, the parathyroid hormone 2 receptor (PTH2R; Faber et al., 2007; Usdin, 2000). TIP39 addition to hypothalamic explants increases CRH, luteinizing hormone-releasing hormone, growth hormone-releasing hormone, and arginine-vasopressin release (Ward et al., 2001), and its intracerebroventricular administration increases circulating ACTH (Ward et al., 2001) and suppresses arginine-vasopressin (Sugimura et al., 2003).

The pathways for TIP39's effects on PVN output are unknown. In rat, somatostatin cells are the only neuroendocrine population labeled by PTH2R antibodies (Dobolyi et al., 2006). However, many hypothalamic PTH2R-ir fibers coexpress vesicular glutamate transporter 2 (VGlut2) in rat (Dobolyi et al., 2006), and we now show this in mouse. Because endogenous glutamate release within the PVN activates the HPA axis and terminals containing VGlut2 contact CRH neurons (Ziegler and Herman, 2000), TIP39 could act via effects on neurotransmitter release from glutamatergic terminals. This study tests that hypothesis. We investigated the relationship among fibers containing TIP39-ir, PTH2R-ir, and glutamate-ir and between PTH2-ir fibers and neuroendocrine cells in the PVN. Because the PTH2R antibody labels fibers and terminals but not cell bodies, we used β -galactosidase immunoreactivity (β -gal-ir) in sections from PTH2R-lacZ knock-in mice (Faber et al., 2007) to identify PTH2R neurons in the PVN region. We marked neuroendocrine cells by peripheral administration of fluorogold, which is taken up by terminals outside the blood-brain barrier (Merchenthaler and Lennard, 1991; Van der Krans, 1983). Synthesis of the PTH2R by glutamatergic neurons within the PVN area and the part of the anterior hypothalamus adjacent to PVN was confirmed by combined in situ hybridization for PTH2R and VGlut2 mRNA. To assess HPA activation by TIP39 and its glutamate dependence, we infused TIP39 into the PVN with or without the ionotropic glutamate receptor blockers DL-2-amino-5-phosphonopentanoic acid (AP-5) and 6-cyano-7-nitroquinoxaline-2,3-dione (CNQX) and measured PVN pCREB-ir and plasma corticosterone. Because the results suggested HPA axis modulation by TIP39, we evaluated basal corticosterone in mice with genetic deletion of TIP39's coding sequence. The results suggest that TIP39 modulates activation of the HPA axis through its effects on glutamatergic interneurons in the PVN area.

MATERIALS AND METHODS

Animals

All procedures were performed according to approved National Institute of Mental Health animal care protocols and in accordance with the Institute for Laboratory Animal Research *Guide for the care and use of laboratory animals*. Development and genotyping of PTH2R-

lacZ knock-in (Faber et al., 2007) and TIP39 knockout (Usdin et al., 2008) mice have been previously described. In the PTH2R lacZ knock-in mice, a cassette encoding β -gal and neomycin phosphotransferase replaces the first coding exon in the PTH2R reading frame. Comparison of either β -gal histochemical reaction product or immunohistochemistry for β -gal with in situ hybridization for PTH2R mRNA shows that β -gal expression matches PTH2R expression (Faber et al., 2007). In these mice β -gal accumulates as extremely fine particles in the cells that synthesize it. The entire coding sequence for TIP39 is replaced by a β -gal/neomycin phosphotransferase cassette in the TIP39 knockout mice (Usdin et al., 2008). TIP39 knockout mice used for the basal corticosterone measurements were backcrossed five times into C57Bl/6J. KO and WT mice were generated from the same heterozygote \times heterozygote matings. A plasmid construct for generation of PTH2R knockout mice was made by homologous recombination in *Escherichia coli* as described by Liu et al. (2003), using reagents provided by Neal Copeland's laboratory (<http://recombineering.ncifcrf.gov/>). Briefly, loxP sites flanking exon 5 and a phosphoglycerate kinase promoter-neomycin resistance sequence were introduced into an approximately 10-kb PTH2R genomic fragment subcloned into a plasmid vector (Fig. 1). After electroporation and growth under selection, SV129Ev/C57Bl/6 F1 hybrid ES cells with homologous recombination were identified by Southern blot. Mice generated from these ES cells were crossed with Cre recombinase deleter mice (O'Gorman et al., 1997) to produce a line with permanent deletion of exon 5. These mice were identified and genotyped by PCR using primers (Pf1, 5'-GGTGTAAGTTATCTGAAGTCACGGG-3'; Pf2, 5'-TTCTCTTCCTCCTCCTCCTAC-3'; Vf1, 5'-TGACCGCTTCCTCGTGCTTT-3'; Pr1, 5'-CCCTGTCTGCTCTTTGCTTACG-3') as indicated in Figure 1. Deletion of PTH2R exon 5 removes a transmembrane domain and introduces a frame shift. This was verified by sequencing RT-PCR products from the brain of knockout mice. DNA sequencing was performed by the NINDS intramural sequencing facility. ES cell and mouse embryo manipulations were performed by the NIMH intramural transgenic core facility. The exon 5 PTH2R knockout mice used in this study were on a mixed SV129Ev/C57Bl/6 background. Mice used for immunohistochemistry (IHC) were between 90 and 150 days old. Mice used for experiments that involved stereotaxic injection were males between 120 and 140 days old (30–32 g).

Antibody characterization

The antibodies against normal mouse proteins used in this study are directed against antigens with well-established neuroanatomical distributions. We confirmed that these distributions were reproduced under the labeling conditions used. Key features of the antibodies used for immunohistochemistry (IHC) are summarized in Table 1.

Arginine-vasopressin—The antibody has been shown to bind specifically to vasopressin-specific neurophysin using radioimmunoassay and Western blotting and by immunohistochemistry to have a labeling pattern consistent with vasopressin in rat (Ben-Barak et al., 1984) and mouse (Zhang et al., 2002) PVN and supraoptic nucleus. Cross-reactivity with mouse vasopressin-associated neurophysin was demonstrated by solid-phase RIA (Ben-Barak et al., 1984).

β -Gal—Antibody specificity was verified by the absence of labeling in WT animals and by labeling with a pattern that matches the expression pattern of the endogenous gene in transgenic knock-in mice (Faber et al., 2007).

CRH—The antibody specifically recognizes rat/human (r/h) CRH demonstrated by RIA and in competition studies with r/h CRF and structurally related peptides (Sawchenko,

1987a,b;Vale et al., 1983). By immunohistochemistry, it labels cells in the mouse PVN (Justice et al., 2008), and in our hands it strongly labeled neuronal fibers in the PVN area.

Fluorogold—Antibody specificity was verified by the absence of labeling in animals not injected with fluorogold and by labeling within the PVN of animals following peripheral administration of fluorogold.

Glutamate—According to the manufacturer, there exists no measurable cross-reactivity (<1:1,000) against glutamate in peptides or proteins. There was no measurable glutaraldehyde-fixed tissue cross-reactivity (<1:1,000) against L-alanine, γ -aminobutyrate, 1-amino-4-guanidobutane, D/L-arginine, D/L-aspartate, L-citrulline, L-cysteine, D/L-glutamine, glutathione, glycine, L-lysine, L-ornithine, L-serine, taurine, L-threonine, L-tryptophan, or L-tyrosine and modest cross-reactivity (1:20) against D-glutamate. There was significant cross-reactivity (1:8) against free N-acetylaspartylglutamate in competition assays. However, it has been reported that N-acetylaspartylglutamate is not retained in aldehyde-fixed tissue.

Oxytocin—The antibody has been shown to bind specifically to oxytocin-specific neurophysin by RIA and Western blotting and by immunohistochemistry to have a labeling pattern consistent with oxytocin (Ben-Barak et al., 1984). We observed immunohistochemical labeling of cells in the mouse PVN and SON (data not shown).

pCREB—A 43-kb band that corresponds to the size of CREB and to the band labeled by another CREB antibody is present on a Western blot from forskolin-treated but not untreated SKNSH cells. Immunohistochemical labeling of tissue sections was blocked in the presence of a phospho-CREB peptide and was eliminated by treatment with a phosphatase inhibitor. The antibody also weakly detects a band in forskolin-treated cells of about 40 kb identified as the phosphorylated form of the CREB-related protein ATF-1 (information from the manufacturer).

PTH2-R—The antibody labels cells transfected with a human PTH2-R cDNA but not the parent cells or cells transfected with a PTH1-R cDNA. Several bands are labeled on Western blots from transfected cells; the highest mobility band (about 85 kD) migrates with same apparent molecular weight as an epitope-tagged receptor. Endoglycosidase digestion reduces the apparent molecular weight to that predicted from the cDNA sequence (about 63 kD). Absorption of a working dilution of antiserum with the peptide used for KLH coupling (10 μ g/ml) eliminates tissue labeling. In rat, the location of cell bodies labeled with the antibody corresponds closely to the location of those labeled with an in situ hybridization probe (Faber et al., 2007; Usdin et al., 1999; Wang et al., 2000).

Somatostatin—The antibody shows no cross-reactivity with enkephalins, other endorphins, substance P, or calcitonin-related protein (manufacturer's information). Preabsorption with 1 μ M somatostatin eliminated tissue staining in rat (Kawaguchi and Shindou, 1998) and with 10 μ g/ml in mouse (Xu et al., 2006). We observed labeling of cells in the mouse hypothalamic periventricular nucleus (data not shown) that corresponded in position to the reported distribution of somatostatin mRNA (Lein et al., 2007).

Thyrotropin-releasing hormone—The antibody was characterized by RIA of synthetic peptides and brain extracts (Wu and Jackson, 1988). On Western blot, it labels bands corresponding to identified processing products of prothyrotropin-releasing hormone of 26 kD, 16.5 kD, and 9.6 kD in AtT20 cells transfected with a preprothyrotropin-releasing hormone cDNA but not control cells (Nillni et al., 1993). By immunohistochemistry, it

labels nerve fibers with a distribution that matches binding of labeled preprothyrotropin-releasing hormone in the rat arcuate nucleus (Goldstein et al., 2007).

TIP39—Antibody specificity was verified by the absence of labeling in mice genetically lacking TIP39 (Fegley et al., 2008) and its presence in WT rats and mice in areas from which it is lost following lesion of regions that contain TIP39-synthesizing neurons (Dobolyi et al., 2003a).

Tyrosine hydroxylase—The antibody has been reported to label all known catecholamine cell groups in rat and to precipitate tyrosine hydroxylase (Semenenko et al., 1986). With the sections used for this study, we observed labeling that corresponded to the well-described rostral periventricular and arcuate hypothalamic groups (Bjorklund and Nobin, 1973).

VGlut2—The antibody recognizes a single band of 50–62 kD on Western blots. PreadSORption with the GST fusion protein used as immunogen, but not a VGlut1 fusion protein, completely abolished immunolabeling. Cells transfected with the cDNA are labeled on Western blots and by immunocytochemistry, and the parent cells and cellstransfected with a VGlut1 cDNA are not (Fremeau et al., 2001). Under the labeling conditions used in this study, strong, punctate labeling was present in most parts of the diencephalon, and much less labeling was present in telencephalic areas, which is consistent with previously described distributions of this transporter (Fremeau et al., 2001; Varoqui et al., 2002).

Identification of neuroendocrine neurons

Six PTH2R-lacZ knock-in mice were injected intraperitoneally with fluorogold (Invitrogen, Carlsbad, CA) dissolved in 0.9% saline at a dose of 15 mg/kg body weight (Merchenthaler and Lennard, 1991). The animals were killed 6 days after the injection, and the brains were processed for β -gal-ir. To obtain good visualization of CRH-containing cell bodies, 2 μ g colchicine dissolved in 5 μ l saline was injected into a lateral ventricle of three mice. The animals were given fluid subcutaneously and killed after 48 hours, and tissue was processed for IHC as described below.

Tissue processing for IHC

Animals were anesthetized with pentobarbital (50 mg/kg i.p.) and transcardially perfused with phosphate-buffered saline, pH 7.4 (PBS), containing 0.1 g procainamide and 5,000 IU heparin per 100 ml solution, followed by cold 4% paraformaldehyde containing 2% acrolein in PBS, pH 7.4. The brains were removed and placed in 4% paraformaldehyde fixative at 4°C overnight and then transferred to PBS. Forty-micrometer-thick coronal sections were cut with a vibrating microtome.

pCREB IHC

After sectioning, free-floating sections were washed with PBS, incubated in 3% H₂O₂ for 15 minutes, and blocked with 2% bovine serum albumin (BSA; ICN Biomedicals, Solon, OH), 0.3% Triton X-100 (Sigma-Aldrich, St. Louis, MO) in PBS for 2 hours, then incubated for 24 hours at 4°C in pCREB antibody. Next, the sections were rinsed with PBS and incubated in biotinylated donkey anti-rabbit antiserum 1:2,500 (Jackson ImmunoResearch, West Grove, PA) for 2 hours at room temperature. After washes with PBS, horseradish peroxidase was introduced with Vectastain Elite ABC reagents 1:500 (Vector Laboratories, Burlingame, CA) for 1 hour. After further rinses with PBS, the sections were incubated with FITC-tyramide (1:10,000) and 0.04% H₂O₂ in 0.1 M Tris solution, pH 7.5, for 10 minutes. Tissue sections were counterstained by incubation in 4',6-diamidino-2-phenylindole (DAPI) solution (5 mg/ml in PBS) for 5 minutes. The sections were then mounted on positively

charged slides and air dried, and coverslips were applied with 2.5% PVA-DABCO (polyvinyl alcohol-1,4-diazabicyclo[2,2,2]octane) antifade mounting medium. Images were captured with a Zeiss Axioplan2 fluorescence microscope and an Axiocam HR (Carl Zeiss, Thornwood NY). Atlas-matched sections were identified from the DAPI counterstaining. Image J software (Rasband, 1997–2009) was used to outline the PVN proper and the peri-PVN zone and to assist with manual counting of the pCREB-ir cells on the side that best matched bregma -0.94 mm as defined in the atlas of Franklin and Paxinos (2008).

Double label IHC

The first step in the double label IHC was labeling for PTH2R-ir. This was executed as for the single label IHC, starting with the PTH2R primary antibody at 1:20,000 dilution. In the second step, the sections were incubated with primary antibodies against VGlut2 (gift from Dr. Robert Edwards, UCSF) or different PVN neuroendocrine markers listed in Table 1. For each antibody, the labeling pattern obtained on our material was the same as that described in the literature for the corresponding antigen. Cross-reactivity between primary antibodies raised in the same species was prevented by application of an antibody-stripping protocol as described by Toth and Mezey (2007). This technique allows for the primary antibodies to be washed off the tissue while leaving the dye-tyramide deposits intact. Briefly, after the conclusion of the staining stage for PTH2-ir, the sections were incubated in 0.01 M citric acid, pH 6.0, at 90 °C for 15 minutes, followed by several rinses in PBS on a rotating platform. After the incubation with the second primary antibody, the sections were incubated with a matching Alexa 594-labeled secondary antibody (Invitrogen) for 3 hours, rinsed with PBS, mounted, and coverslipped with 2.5% PVA-DABCO. Controls were performed with each antibody-stripping procedure to ensure that primary antibodies from previous steps did not contribute detectable signal.

Double label IHC for β -gal and fluorogold after intraperitoneal injection of the retrograde tracer was performed with chicken β -gal antibody, and the signal was developed by tyramide amplification with Pacific blue-tyramide as the fluorochrome as described above for other immunolabeling. Some fluorogold-containing material was labeled with rabbit antifluorogold serum and Alexa 594-labeled anti-rabbit secondary antibody.

Triple label IHC

After the blocking step, the free-floating sections from four mouse brains were incubated in CRH primary rabbit antibody at 1:1,000, followed by the amplification protocol with anti-rabbit biotinylated antiserum as described for single label IHC. The same immunolabeling procedure was applied two more times with rabbit primary antibodies to the PTH2R at 1:3,000 dilution and TIP39 at 1:1,000 dilution. To avoid cross-reactivity, each step of immunolabeling was followed by antibody stripping as described above. The fluorescent dyes used were DyLight 405-tyramide for TIP39, DyLight 488-tyramide for PTH2R, and DyLight 594-tyramide for CRH. In the final step, after washes with 0.1 M Tris, pH 7.5, the sections were mounted on positively charged slides, air dried, and coverslipped with 2.5% PVA-DABCO mounting medium.

Assessment of immunohistochemistry

The anatomical level of sections through the PVN was identified using the Franklin and Paxinos (2008) atlas. Immunolabeling was visualized in representative sections with a Zeiss LSM 510 confocal microscope in the NINDS Intramural Light Imaging Facility. Z series were analyzed in Volocity software (Improvision, Waltham MA). Parameters for the PTH2R/neuroendocrine marker Z series were $1,024 \times 1,024 \times 15$, scaling $0.14 \mu\text{m} \times 0.14 \mu\text{m} \times 0.5 \mu\text{m}$, $\times 63$ oil, wavelengths 488 nm and 543 nm. Areas of apparent contact between PTH2R-ir processes and processes and cells immunoreactive for neuroendocrine markers

were identified with the following procedure. After automated thresholding of the individual channels, objects less than $0.25 \mu\text{m}^3$ were excluded from the PTH2R channel and less than $0.5 \mu\text{m}^3$ from the neuroendocrine marker channel; areas above threshold in the PTH2R channel that did not also contain suprathreshold labeling in the neuroendocrine channel were excluded, and the remaining areas were pseudocolored yellow. The images in Figure 5 are single optical sections from the Z-stack used for analysis.

Double label fluorescent in situ hybridization histochemistry

Initial stages of tissue preparation and probe hybridization were performed as described previously for radioactive in situ hybridization (Faber et al., 2007). Briefly, 12- μm -thick coronal sections were cut through the hypothalamus from unfixed rapidly frozen brains, thaw mounted onto positively charged slides, and stored -80°C until hybridization. Slide-mounted sections were fixed in 4% paraformaldehyde, rinsed in PBS at 4°C , treated with 0.25% acetic anhydride, pH 8.0, rinsed in $2\times$ standard saline citrate (SSC; 175.3g NaCl and 88.2 g Na citrate in 1 liter H_2O), and then dehydrated with ethanol and delipidated with chloroform/ethanol. Sections were prehybridized in hybridization mix containing a final concentration of 50% formamide, 10% dextran sulfate, 0.3 M NaCl, 10 mM Tris, 1 mM EDTA, $1\times$ Denhardt's solution, and 10 mM DTT.

PCR products synthesized with T7 RNA polymerase recognition sites incorporated into the antisense strand corresponding to bases 1426–2040 of the mouse PTH2R (Genbank accession AK045576) and bases 2132–2558 of mouse VGlut2 (Genbank accession NM_080853) were used as probe templates. Riboprobes were synthesized using T7 RNA polymerase from a Maxiscript kit (Ambion, Austin TX) and RNA Labeling Mix (Roche Diagnostics, Mannheim, Germany) with biotin-UTP for the PTH2R probe and digoxigenin-UTP for the VGlut2 probe following the manufacturer's instructions and purified by using gel filtration spin columns. PTH2R and VGlut2 probes (final concentration 10 ng/ μl each) and 0.25 $\mu\text{g}/\text{ml}$ salmon sperm DNA were added to hybridization mix and incubated on the slide-mounted sections under coverslips overnight at 55°C . After the incubation, the coverslips were rinsed off with $1\times$ SSC, and the slides were incubated in RNase solution (RNase A 10 mg/ml, 0.5 M NaCl, 10 mM Tris-HCl, 0.5 mM EDTA) at 37°C for 30 minutes. After that, the sections were washed with $0.1\times$ SSC four times for 15 minutes each at 65°C , followed by a 1-hour wash at room temperature in $1\times$ SSC.

To detect the hybridized probes, the slides were incubated in 3% hydrogen peroxide/0.2% sodium azide solution for 15 minutes, thoroughly rinsed in 0.1 M Tris, pH 7.5, and blocked in 2% BSA/0.3% Triton X-100 solution in 0.1 M Tris, pH 7.5, for 1 hour. After the blocking step, the sections were incubated for 1 hour with sheep antidigoxigenin Fab fragments conjugated with horseradish peroxidase (catalog No. 11 633 716 001; Roche Diagnostics) diluted 1:1,000, followed by incubation with Pacific blue-tyramide (1:8,000) and 0.04% H_2O_2 in 0.1 M Tris (pH 7.5) for 30 minutes. This was followed by overnight incubation with mouse antibiotin DyLight 594 antibody (catalog No. 200-512-211; Jackson Immunoresearch), 1:1,000 dilution in 0.1 M Tris. To confirm the specificity of the fluorescent signal, negative controls without probes were put through the same in situ hybridization and immunolabeling steps. For precise assessment of PTH2R mRNA distribution in the hypothalamus, single PTH2R mRNA-labeled sections with FITC-tyramide instead of Pacific blue-tyramide were counterstained with DAPI. The sections were air dried and mounted with PVA-DAPCO antifade medium. Tyramide derivatives of fluorescent dyes were synthesized as described by Hopman et al. (1998) by using succinimidyl-coupled carboxyfluorescein (Sigma, St. Louis, MO), Pacific blue, and Alexa dyes (Invitrogen, Carlsbad, CA) or DyLight dyes (Fisher Scientific, Pittsburg PA).

Coronal brain sections were atlas-matched according to the mouse brain atlas of Franklin and Paxinos. Images of the PVN area were acquired with 405-nm and 543-nm lasers on a Zeiss LSM 510 confocal microscope. The tissue background permitted visualization of landmarks, including the compact cell mass of the PVN with the magnocellular subdivision, fornix, optic tract, and third ventricle. Images covering the entire PVN were collected from two sections per animal at level -0.94 mm to bregma, and the number of labeled and double-labeled cells was manually counted on one side that matched the desired level. The mean number of labeled neurons was calculated for the areas of interest.

Preparation of figures

Images were digitally captured with cameras and software on the specific instruments described above. Image processing was performed in Image J or Volocity software as described. Images were imported into Adobe Photoshop, cropped, adjusted for optimal contrast using the “Levels” command, and in some cases colors were altered by pasting entire images into selected channels and by using the “Selective colors” command. No manipulations of individual image elements were performed.

Implantation of PVN cannulae

Male mice, 120–140 days old, 30–32 g in weight, were anesthetized with isoflurane and placed in a stereotaxic apparatus. Bregma and lambda were identified from skull sutures exposed following longitudinal skin incisions and removal of pericranial connective tissue. A double 26-gauge stainless steel guide cannula (Plastics One, Roanoke, VA) was implanted into the PVN (anteroposterior -0.8 mm, lateral ± 0.2 mm, and dorsoventral -4.0 mm from bregma). The cannulae were secured to the skull with three screws and acrylic dental cement. Stylets were placed in each cannula to maintain patency. Animals were handled daily, and the stylets were manipulated to acclimate the animals to the microinjection procedure and to reduce tissue growth on the cannulae tips.

Drug infusion

On the day of the experiment, the animals were brought to the procedure room to acclimate to the surroundings. After 1 hour, 33-gauge internal injectors extending 0.5 mm beyond the tip of the guide cannula were inserted. A cannula connector was used to attach the injectors to a syringe pump for delivery of equal volumes of 0.5 μ l vehicle per side (0.1% BSA in 0.9% saline), 100 pmol of TIP39 (custom synthesis by Midwest Biomedicals, Mokena, IL), or a cocktail of 100 pmol TIP39, 30 pmol CNQX, and 30 pmol AP-5 (Tocris Bioscience, Ellisville, MO) into the PVN over a period of 10 minutes. Five hours after the insertion of the injectors, between 1200 and 1400 hours, the predetermined amount of fluid was injected. The injectors remained in place for the duration of the experiments. Blood samples of 0.2 ml were collected in cold microcentrifuge tubes containing 10 μ l of 0.5 M EDTA 15 minutes after drug infusion by piercing the submandibular vascular plexus with a lancet. Blood was centrifuged for 20 minutes at 1,800 rpm; the plasma was collected and frozen (-20°C) until determination of corticosterone and prolactin levels. Immediately after the blood collection, the animals for pCREB immunostaining were deeply anesthetized and perfused with fixative. Probe placement was verified histologically, and only those animals with cannulae inserted just above the PVN were included in the study.

To assess the effective diffusion of TIP39 under the experimental conditions, a single 26-gauge cannula was implanted in a group of six animals. In two animals, cannulae were positioned directly above the PVN; in two, the cannulae were positioned 0.5 mm laterally from the coordinates used for the PVN, and two animals were implanted with cannulae 0.5 mm laterally to the second set of cannulae or at a distance of 1 mm from the PVN. After 6 days, each animal received an infusion of 0.5 μ l, containing 100 pmol TIP39. The mice were

killed and perfused 15 minutes after the infusion, and alternating adjacent sections through the PVN were immunolabeled for p-CREB-ir or PTH2R-ir. To evaluate the diffusion distance of TIP39, 0.5 μ l fluorescent-labeled TIP39 (prepared by addition of excess carboxyfluorescein succinimide to a 1 mM TIP39 solution, followed by dialysis against PBS) was injected into the PVN of four mice. The animals were killed and perfused with fixative 15 minutes after the infusion. Forty-micrometer sections were cut and fluorescent and brightfield images obtained.

Radioimmunoassay

Plasma corticosterone levels were measured using the ImmuChem Double Antibody 125 I RIA kit manufactured by MP Biomedicals (Orangeburg, NY). All samples from each experiment were processed together, and the sensitivity of the assay was 7.7 ng/ml. Mouse prolactin RIA was performed by Dr. Albert Parlow, National Hormone and Peptide Program, University of California, Los Angeles.

Statistical analysis

Data are reported as mean \pm SEM. Data were analyzed by Student's *t*-test or two-way ANOVA followed by Student-Newman-Keuls test. The results were considered significantly different at $P < 0.05$.

RESULTS

PTH2R and VGlut2 double labeling by immunohistochemistry and in situ hybridization

Double immunolabeling for PTH2R-ir (Fig. 2A) and VGlut2-ir (Fig. 2B) revealed a high level of coexpression between PTH2R-ir fibers and VGlut2-ir puncta in the PVN and the adjacent area (Fig. 2C). In situ hybridization with a PTH2R probe detected by fluorescent labeling showed a distribution like that previously described using a radioactive in situ hybridization probe (Faber et al., 2007) and observed with immunohistochemistry for β -gal in PTH2R lacZ knock-in mice (Faber et al., 2007, and see below). In the PVN, signal for PTH2R mRNA was present in the anterior, medial, and lateral parvocellular and to some extent in the dorsal capsular subnuclei (Fig. 2D–F). The area of the magnocellular cell group contained only few scattered cells with signal for PTH2R mRNA (Fig. 2D–F). There was a high level of coexpression between PTH2R mRNA and VGlut2 mRNA (example in Fig. 2G–I). To assess the coexpression between PTH2R and VGlut2 mRNA, we set as a criterion for identification of a marker the presence of two or more labeled puncta, like those shown in Figure 2G–I, in a region that could be identified as a cell body based on background nonspecific labeling. By this criterion there were 97 ± 6 PTH2R mRNA-expressing cells per hemisection in the PVN at the level selected for analysis, and $41.8\% \pm 9.1\%$ of them coexpressed VGlut2 mRNA. Among the 67 ± 4 VGlut2 mRNA-expressing cells per hemisection in the same location, $89.3\% \pm 4.7\%$ coexpressed PTH2R mRNA ($n = 4$ animals). The density of PTH2R mRNA-expressing cells was greatest in the central and ventral parts of the anterior hypothalamic area, and the number of labeled cells gradually decreased laterally, and then they completely disappeared in the lateral hypothalamus. In the anterior hypothalamic area that surrounds the PVN and extends to the medial border of fornix, an average of $65\% \pm 1.8\%$ of the counted 111 ± 9 PTH2R mRNA-expressing cells per hemisection also coexpressed VGlut2 mRNA. Among the counted 73 ± 3 VGlut2 mRNA labeled neurons per hemisection in this anterior hypothalamic area, an average of $85.3\% \pm 4.8\%$ coexpressed PTH2R mRNA ($n = 4$ animals). The distribution of PTH2R mRNA in the PVN area and anterior hypothalamus as detected by in situ hybridization with a 35 S-UTP-labeled riboprobe showed the same distribution in the PVN area as the fluorescent riboprobe (Supporting Information Fig. 1).

Labeling with antibodies against TIP39, PTH2R, and glutamate and peripheral tracer labeling of neuroendocrine cells in the PVN

Immunolabeling showed PTH2R-ir fibers throughout the PVN (Fig. 3A). TIP39-ir fibers had a distribution very similar to that of PTH2R-ir (Fig. 3B). Both covered the entire PVN, with the exception of a region of densely packed cells toward the center of the nucleus, and spread laterally into the immediately adjacent anterior hypothalamic area as far as the fornix. Glutamate-ir fibers were present throughout the region occupied by TIP39-ir and PTH2R-ir fibers and occupied a somewhat larger territory (Fig. 3C).

To define further the PTH2R-expressing cells in the PVN area, we used β -gal-ir in PTH2R-lacZ knock-in mice to identify their location (Fig. 3D–F). We performed intraperitoneal injections with fluorogold, a retrograde tracer taken up by nerve terminals outside the blood–brain barrier. Fluorogold labeled numerous neuroendocrine neurons in the PVN, including parvocellular and magnocellular neurons throughout anterior to posterior extent of the PVN (Fig. 3D–F). Most of the β -gal immunoreactivity in the anterior hypothalamus was present in a rim around the endocrine PVN at a distance of 50–100 μ m from the edge of the nucleus as defined by the fluorogold-labeled cells (Fig. 3D–F). There were also a number of β -gal-ir neurons dispersed among the PVN neuroendocrine cells as well as in the hypothalamic periventricular nucleus, but we found very few convincing examples of fluorogold tracer and β -gal-ir labeling of the same cells. Almost all of the β -gal-ir signal was not from the neuroendocrine cells [Fig. 3G–I; Supporting Information Fig. 2 shows the tissue background from a WT (lacZ⁻) animal].

Triple label IHC with antibodies against PTH2R-, TIP39-, and CRH-ir in the PVN

PTH2R-ir and TIP39-ir fibers covered all anatomical subdivisions of the PVN (Fig. 4A,B). As in the previous labelings, TIP39-ir fibers appeared somewhat thicker than PTH2R-ir fibers. CRH-ir neurons had a distribution similar to that previously described for colchicine-treated mice (Alon et al., 2009). High-power confocal images showed both PTH2R-ir and TIP39-ir fibers juxtapositioned around CRH-ir cells (Fig. 4E–H). The two types of fiber were never observed to colocalize despite their robust expression levels and their close proximity, even when surrounding the same CRH-ir neuron (Fig. 4E–H).

IHC for PTH2R-ir and neuroendocrine markers in the PVN

Antibodies recognizing tyrosine hydroxylase, oxytocin, arginine-vasopressin, CRH, thyrotropin-releasing hormone, and somatostatin labeled cell bodies and fibers with their expected anatomical distribution. With *touching* defined as approaching within a distance less than the imaging technique's resolution, which was approximately 0.14 μ m, PTH2R-ir fibers touched parts of cell bodies or fibers containing each of these markers (Fig. 5). In most cases it was also clear that PTH2R-ir was not in the same structure as the neuropeptide or tyrosine hydroxylase, because only parts of each labeled structure touched. The highest level of colocalization was observed between PTH2R-ir fibers and thyrotropin-releasing hormone-ir (Fig. 5E) or somatostatin-ir (Fig. 5F) cell bodies and fibers. Despite the poor visualization of CRH-ir cell bodies in the brain sections from non-colchicine-treated mice (four or five cells per brain), all of the observed CRH-ir neurons had adjacent PTH2R-ir fibers. The multiple CRH-ir neurons visible after colchicine treatment did not differ in their PTH2R-ir innervation (Fig. 6).

Expression of pCREB-ir after infusion of TIP39 with or without ionotropic glutamate receptor blockers

The anatomical data suggest that TIP39-containing nerve terminals are adjacent to glutamatergic nerve terminals that contain PTH2Rs (Figs. 2, 4) and that these PTH2R-ir

terminals closely appose neuroendocrine cells (Fig. 5), including CRH-ir neurons (Figs. 4, 6). TIP39 was infused into the PVN area to investigate whether glutamatergic transmission is required for TIP39 activation of neuroendocrine cells.

The effects of the infusions were evaluated after confirmation of appropriate cannula placement (Fig. 7A). Infusion of 0.5 μ l vehicle or the same volume of vehicle containing 30 pmol CNQX and 30 pmol AP-5 had little overall effect on pCREB expression. A few cells expressing pCREB-ir were evenly scattered in the PVN and the surrounding anterior hypothalamus. The unstimulated PVN had a slightly higher number of activated cells than the adjacent structures. (Fig. 7B,F–H). Fifteen minutes after infusion of 100 pmol TIP39 into the PVN, pCREB-ir expression was obvious in an area that extended about 0.5 mm from the cannula tips on each side of the third ventricle. Activated neurons were present in the periventricular nucleus medially, the anterior hypothalamic area adjacent to the PVN almost as far laterally as the fornix, and as a thin rim of activation just above the dorsal edge of PVN (Fig. 7C,F,H). Most of the pCREB-expressing cells were in the PVN, where the number of activated neurons was twice the number of cells expressing pCREB with vehicle infusion. The activated cells formed a compact mass, with the shape of the PVN. There was no obvious difference in pCREB-ir expression between the parvocellular and magnocellular subdivisions of the nucleus. Increased pCREB-ir was also clearly visible in a 40–50- μ m-wide peri-PVN zone of the anterior hypothalamus that immediately surrounds the PVN. This region contained approximately one-third of the pCREB-ir cells following TIP39 infusion (Fig. 7C,H). pCREB-ir cells in the peri-PVN zone increased by 110.8%, and pCREB-ir cells in the PVN increased by 91.8% after the infusion, or the total number of activated cells in the TIP39-injected group increased by about 98.7% in comparison with the control group (Fig. 7). The expression of pCREB in the SON and the lateral hypothalamic area did not increase over baseline with TIP39 infusion. Other brain areas known to express PTH2Rs, including the cerebral cortex, lateral septum, and amygdala, also did not have increased levels of pCREB-ir.

Infusion of a cocktail containing TIP39, CNQX, and AP-5 did not significantly increase the number of pCREB-ir cells (Fig. 7D,F–H). The number of pCREB-ir cells in PTH2R knockout mice following TIP39 infusion was also very similar to the number in the vehicle-treated control group (Fig. 7F–H). Although this did not reach statistical significance, the CNQX/AP-5-treated group had the lowest absolute number of pCREB-ir cells (Fig. 7F–H).

To address the potential concern that PVN neurons could be unexcitable in the presence of the ionotropic-glutamate receptor antagonists, because of either damage or unopposed GABA inhibition, we pinched a hind leg with forceps immediately after the infusion of TIP39/CNQX/AP-5 in one group of animals. This mild sensory stressor activates PVN neurons mainly via norepinephrine transmission (Palkovits et al., 1999; Smith and Day, 1994). pCREB-ir expression in this group of animals was increased exclusively in the PVN, and the number of activated cells was not statistically different from the number of pCREB-expressing cells 15 minutes after TIP39 infusion (Fig. 7E–H). However, pCREB-ir expression in the perinuclear zone surrounding PVN was very similar to the expression of the control groups (Fig. 7H).

To examine the effective spread of TIP39 under the experimental conditions, 0.5 μ l (100 pmol) TIP39 was infused via single cannulae placed at several sites within the hypothalamus, and the animals were killed after 15 minutes. There was no increase in pCREB immuno-reactivity from cannulae terminating more than 1.0 mm from the PVN (Fig. 8). Infusion of the same volume of fluorescent TIP39 into the PVN also indicated an effective diffusion radius of about 0.5 mm, 15 minutes following injection of 0.5 μ l peptide (Fig. 8H–J). These results are very similar to the previously described detectable diffusion of

about 1 mm in rat brain following infusion of 0.5 μ l of dyes with molecular weight less than 1,000 (Myers, 1966).

Plasma levels of corticosterone and prolactin after TIP39 infusion

Plasma corticosterone was 250.2 ± 47.7 ng/ml 15 minutes after infusion of 100 pmol TIP39 into the PVN vs. 43.7 ± 16.2 ng/ml in the vehicle-treated control group ($n = 4/7$; Fig. 9). The same amount of TIP39 injected into PTH2R knockout mice did not significantly increase plasma corticosterone level. The plasma corticosterone levels also did not increase above baseline in animals administered vehicle/CNQX/AP-5 or TIP39/CNQX/AP-5. The corticosterone level increased to 190 ± 27.6 ng/ml in the group that received a hind leg pinch after the infusion of the TIP39/CNQX/AP-5 mixture, which was not significantly different from the TIP39-injected group but was significantly higher than control animals (Fig. 9A). In the same blood samples, administration of TIP39 significantly decreased the plasma prolactin level (100 pmol TIP39 1.7 ± 0.4 ng/ml vs. vehicle control 11.4 ± 3.2 ng/ml, $n = 4 / 7$). A slight decrease of plasma prolactin levels in the other groups did not reach statistical significance (TIP39/PTH2RKO 6.6 ± 2.6 ng/ml, vehicle/CNQX/AP-5 4.6 ± 1.9 ng/ml, TIP39/CNQX/AP-5 4.7 ± 1.2 ng/ml, and TIP39/CNQX/AP-5/pinch 5.6 ± 1.1 ng/ml; Fig. 9B).

Plasma corticosterone concentration in TIP39-KO mice

Basal corticosterone levels were slightly lower in TIP39 knockout mice than in WT controls. The difference reached statistical significance in samples obtained near the time when mice were expected to have their peak corticosterone level but not in the samples obtained near the expected trough. One hour before the lights-on phase of the day, TIP39 knockout corticosterone was 13 ± 3.4 ng/ml and wild-type was 8.7 ± 7 ng/ml. One hour before the lights-off phase of the day, in the same group of animals tested 7 days previously, corticosterone was 66.3 ± 9.3 ng/ml in the TIP39 knockout vs. 88.4 ± 13.1 ng/ml in the wild-type mice ($P < 0.01$, $n = 8/13$ group; Fig. 10).

DISCUSSION

The major finding of this study is that TIP39 activates hypothalamic neuroendocrine cells in a PTH2R- and an ionotropic glutamate receptor-dependent manner. This was observed as an increase in the number of pCREB-ir positive cells, an increase in plasma corticosterone, and a decrease in plasma prolactin following TIP39 infusion into the PVN area. In combination with the presence of TIP39-containing fibers in many parts of the anterior hypothalamus and PTH2R immunoreactivity on glutamatergic neurons in the PVN as well as the PTH2R-ir fibers seen in close apposition to, or touching, parts of each of the principal neuroendocrine cell types present in the PVN, the data strongly suggest that TIP39 normally modulates excitation of neuroendocrine cells via effects on local nonendocrine excitatory neurons. The high level of PTH2R mRNA expression by the VGlut2 mRNA-expressing neuronal population of the PVN and adjacent hypothalamic area also supports the suggestion that TIP39 can alter the activity of the local glutamatergic network. A modulatory influence of TIP39 on HPA axis status is also suggested by a small decrease in the level of corticosterone near the time of its expected physiological peak in TIP39 knockout mice.

PTH2 receptors are present on local glutamatergic neurons in the PVN region

Immunohistochemistry showed fibers containing PTH2R-ir and glutamate-ir throughout the PVN. In many cases, both labels could be followed along the same individual fibers. Despite the fact that glutamate is a ubiquitous amino acid, immunolabeling with an antibody to glutamate has been used in a number of studies to identify glutamatergic neurons (Chagnaud et al., 1989; van den Pol and Trombley, 1993; van den Pol et al., 1990). This may be

effective because of the relatively high concentration of glutamate in synaptic vesicles and either a low background from, or loss of, cytoplasmic glutamate during tissue processing. We previously described extensive colocalization between PTH2R-ir and VGlut2-ir in the hypothalamus in rat (Dobolyi et al., 2006), and we have now shown that this is also the case in the mouse PVN area. In addition, we used dual in situ hybridization with PTH2R and VGlut2 probes to show that the majority of cells that express either of these mRNA's in the PVN area express both. Thus, it is likely that most PTH2R-containing fibers in the PVN area are the processes of glutamatergic neurons.

Forty-three percent of PVN synaptic boutons are reported to have local, interneuronal origin (Kiss et al., 1983), and some of them are glutamatergic (Csaki et al., 2000; van den Pol and Trombley, 1993). Effects on magnocellular neurons mediated by glutamatergic interneurons have been described (Daftary et al., 1998; Ferguson et al., 2008). Several investigators have described glutamatergic terminals in close apposition with neuroendocrine neurons in the PVN (Herman et al., 2003; van den Pol et al., 1990; Wittmann et al., 2005), but the relative contributions of distant and local glutamatergic neurons are not clear. Our experiments show that PTH2R-expressing neurons that contact neuroendocrine cells are probably part of the local glutamatergic interneuron population. Consistent with this view, significant coexpression was not found between PTH2R neurons as marked by β -gal-ir in PTH2R-lacZ knock-in mice and fluorogold taken up following its peripheral injection, which labels neuroendocrine cells. β -Gal is not an ideal marker, insofar as low levels are sequestered in a small intracellular compartment, and we cannot exclude the possibility that it underestimates the number of PTH2R-expressing cells. We believe that the low level of expression results from use of the endogenous promoter to drive expression. Additional evidence for the lack of PTH2R expression by neuroendocrine cells is provided by double immunolabeling. In addition to the lack of colocalization in the PVN, somatostatin was the only neuroendocrine peptide found coexpressed with PTH2R-ir when double labeling was examined in the median eminence, where the PTH2R antibody produces strong labeling of fibers (Dobolyi et al., 2006). Thus, the few PTH2R cells labeled with fluorogold in the paraventricular nucleus are very likely somatostatin-containing neurons. The large number of glutamatergic neurons with PTH2R expression (~90% of VGlut2 mRNA expressing neurons in the hypothalamic areas investigated contained PTH2R mRNA) suggests that the PTH2R plays a significant role in the function of the local glutamatergic network, although it should be noted that the PTH2R is only one of many receptors expressed by these cells. The PTH2R mRNA-expressing cells not found to coexpress VGlut2 mRNA could potentially be a part of the VGlut1 neuronal population in the area. This population, albeit small, is readily detectable in the anterior hypothalamus and PVN (Ziegler et al., 2002). The nondouble-labeled cells could also reflect a limitation of the double labeling method, which used relatively thin (12 μ m) sections. The large number of cells expressing PTH2R mRNA in this region suggests that much of the PTH2 receptor in the PVN area is synthesized by local neurons.

TIP39 activation of neuroendocrine cells through PTH2R/glutamatergic neurons

TIP39-containing fibers are abundant in the neuroendocrine hypothalamus. The distribution of TIP39 fibers is extremely similar between rat and mouse, as is the distribution of TIP39 neurons (Faber et al., 2007), and we previously showed that in rat the hypothalamic TIP39 fibers and terminals are projections from subparafascicular area TIP39 neurons (Dobolyi et al., 2003a). These TIP39 fibers intermingle with a dense network of PTH2R-ir fibers throughout the PVN and adjacent areas (Faber et al., 2007). Data from this study show close apposition between these PTH2R-ir fibers and each of the major neuroendocrine cell types in the PVN, including CRH-ir neurons, indicating that they have the potential for synaptic connectivity. Activation of cells throughout the PVN and the immediately adjacent hypothalamic area following local infusion of TIP39, detected by increased pCREB-ir,

suggests that endogenous TIP39 contributes to activation of these cells. The pattern of pCREB-ir following TIP39 infusion, with indistinct borders and a broad distribution, did not target any specific subnuclei or a particular PVN cell population, which is consistent with the distribution of TIP39- and PTH2R-containing fibers. The robust pattern of neuronal activation suggests that the TIP39/PTH2R system provides a stimulatory influence on multiple neuroendocrine pathways.

Blockade of TIP39-stimulated pCREB-ir and plasma corticosterone by ionotropic glutamate receptor antagonists indicates that the neuronal activation and the associated increase in blood corticosterone concentration are consequences of glutamate release. The PTH2R and TIP39 terminals are ideally positioned to modulate glutamate release from terminals adjacent to neuroendocrine cells. The most parsimonious explanation for the site of TIP39 effect on PVN neuroendocrine cell activation is the PTH2R/glutamate containing terminals that are adjacent to the neuroendocrine cells, although the presence of PTH2Rs and TIP39 fibers in other regions that influence PVN neuroendocrine function indicates that TIP39 could also act less directly.

The mild pain caused by hind leg pinch activates the HPA axis through the sensory spinothalamic pathway (Burstein et al., 1990), in which noradrenergic transmission plays a major role (Palkovits et al., 1999; Smith and Day, 1994). This sensory stimulation increased blood corticosterone in mice that had received glutamate receptor blockers, showing that the blockers did not prevent ACTH secretagogue release. A difference between the TIP39 and noradrenergic activation of the HPA axis under glutamate blockade is that TIP39 infusion increased corticosterone levels while at the same time suppressing plasma prolactin. This decrease in plasma prolactin concentration can be attributed to an effect of TIP39 on a specific set of neurons and not to a general consequence of glutamate or norepinephrine release, because norepinephrine and glutamate (Bregonzio et al., 1998; Kapoor et al., 1993; Nagy et al., 2005; Pohl et al., 1989) increase prolactin secretion when directly infused into the central nervous system. Prolactin secretion is under diverse and complex regulation exerted by the dopamine neurons in the arcuate nucleus (Christian et al., 2007; Kawano and Daikoku, 1987; Meites, 1977), some PVN neuropeptides including vasoactive intestinal polypeptide (Mezey and Kiss, 1985) and thyrotropin-releasing hormone (Fjeldheim et al., 2005), and some classical neurotransmitters such as glutamate (Bregonzio et al., 1998) and serotonin (Rittenhouse et al., 1993). The infusion of TIP39 into the PVN does not permit identification of the exact pathway of prolactin inhibition, but it very likely involves indirect or direct activation of dopamine neurons in the arcuate nucleus.

Implications for TIP39's role in neuroendocrine function

The difference in blood corticosterone levels between wild-type and TIP39 knockout mice observed 1 hour before dark suggests that the TIP39/PTH2R system has an ongoing stimulatory influence on the HPA axis. This study and a previous study (Fegley et al., 2008) did not find a significant difference in basal corticosterone level between WT and TIP39 knockout mice during the inactive (light) phase of the day, when the blood corticosterone levels are at their nadir. The small suppression of the normal rise in corticosterone 1 hour before the active (dark) phase of the day in TIP39-KO mice, in combination with a stress response indistinguishable from that of WT mice following restraint, swim, or audiogenic stress (Fegley et al., 2008), suggests that, in TIP39 knockout mice, the loss of TIP39's normal effect may be overwhelmed by strong stressors. TIP39 may have a modulatory effect on the HPA axis, and perhaps other neuroendocrine systems, which is most obvious when superimposed on modest stimuli. Reduced corticosterone might have been apparent near the daily peak because TIP39 plays a role in the normal endogenous pattern of secretion or because of a favorable signal-to-noise ratio at that corticosterone level. It is possible that the effect observed in TIP39 knockout mice reflects a developmental compensation in this

global knockout. Additional types of experiment are required to investigate more thoroughly the physiological functions of endogenous TIP39.

A stress-dependent increase in anxiety-like behavior in TIP39 knockout mice (Fegley et al., 2008) suggests that TIP39 normally limits the behavioral response to some stressors and that under some circumstances it could be an endogenous anxiolytic activity. Exogenous TIP39 infused into the PVN seemed to stimulate simultaneously ACTH secretagogue(s) and prolactin release inhibitor(s). Whether endogenous TIP39 has both actions simultaneously must depend on whether the TIP39 neurons that reach the relevant populations of PVN cells are the same or under the same influences. The effects of TIP39 also must depend on the activity within the specific circuits with outputs modulated by TIP39 at the time when TIP39 is released.

The data presented here indicate that TIP39 is a specific activator of the HPA axis via local PVN PTH2R-expressing glutamatergic interneurons. The subparafascicular area, which contains the TIP39 neurons that innervate the hypothalamus (Dobolyi et al., 2003b; Wang et al., 2006b), receives cortical, subcortical, and hypothalamic projections (Wang et al., 2006a) that contain information that TIP39 neurons may integrate and transmit to the neuroendocrine hypothalamus. The thalamic PVN also contains cells that project to the hypothalamic periparaventricular region and are thought to be involved in stress integration (Hsu and Price, 2009; Moga et al., 1995). Thus, the TIP39 ligand–PTH2 receptor system appears to be a dynamic contributor to neuroendocrine regulation by the PVN and potentially other hypothalamic areas.

Supplementary Material

Refer to Web version on PubMed Central for supplementary material.

Acknowledgments

We thank Jonathan Kuo, Milan Rusnak, and Jim Pickel and the NIMH transgenic mouse core facility along with the NINDS intramural DNA sequencing facility for invaluable support and Harold Gainer and Eva Mezey for comments on an earlier version of the manuscript.

Grant sponsor: Intramural Program of the National Institute of Mental Health, NIH; Grant number: ZIA MH002685-16.

LITERATURE CITED

- Alon T, Zhou L, Perez CA, Garfield AS, Friedman JM, Heisler LK. Transgenic mice expressing green fluorescent protein under the control of the corticotropin-releasing hormone promoter. *Endocrinology*. 2009; 150:5626–5632. [PubMed: 19854866]
- Ben-Barak Y, Russell JT, Whitnall M, Ozato K, Gainer H. Phylogenetic cross-reactivities of monoclonal antibodies produced against rat neurophysin. *Cell Mol Neurobiol*. 1984; 4:339–349. [PubMed: 6085284]
- Bjorklund A, Nolin A. Fluorescence histochemical and microspectrofluorometric mapping of dopamine and noradrenaline cell groups in the rat diencephalon. *Brain Res*. 1973; 51:193–205. [PubMed: 4706010]
- Boudaba C, Szabo K, Tasker JG. Physiological mapping of local inhibitory inputs to the hypothalamic paraventricular nucleus. *J Neurosci*. 1996; 16:7151–7160. [PubMed: 8929424]
- Bregonzio C, Navarro CE, Donoso AO. NMDA receptor antagonists block stress-induced prolactin release in female rats at estrus. *Eur J Pharmacol*. 1998; 350:259–265. [PubMed: 9696416]
- Brown EM, Segre GV, Goldring SR. Serpentine receptors for parathyroid hormone, calcitonin and extracellular calcium ions. *Baillieres Clin Endocrinol Metab*. 1996; 10:123–161. [PubMed: 8734454]

- Burstein R, Cliffer KD, Giesler GJ Jr. Cells of origin of the spinothalamic tract in the rat. *J Comp Neurol*. 1990; 291:329–344. [PubMed: 2298937]
- Chagnaud JL, Campistron G, Geffard M. Monoclonal antibody directed against glutaraldehyde conjugated glutamate and immunocytochemical applications in the rat brain. *Brain Res*. 1989; 481:175–180. [PubMed: 2565132]
- Charmandari E, Tsigos C, Chrousos G. Endocrinology of the stress response. *Annu Rev Physiol*. 2005; 67:259–284. [PubMed: 15709959]
- Christian HC, Chapman LP, Morris JF. Thyrotrophin-releasing hormone, vasoactive intestinal peptide, prolactin-releasing peptide and dopamine regulation of prolactin secretion by different lactotroph morphological subtypes in the rat. *J Neuroendocrinol*. 2007; 19:605–613. [PubMed: 17620102]
- Cole RL, Sawchenko PE. Neurotransmitter regulation of cellular activation and neuropeptide gene expression in the paraventricular nucleus of the hypothalamus. *J Neurosci*. 2002; 22:959–969. [PubMed: 11826124]
- Csaki A, Kocsis K, Halasz B, Kiss J. Localization of glutamatergic/aspartatergic neurons projecting to the hypothalamic paraventricular nucleus studied by retrograde transport of [³H]D-aspartate autoradiography. *Neuroscience*. 2000; 101:637–655. [PubMed: 11113313]
- Daftary SS, Boudaba C, Szabo K, Tasker JG. Noradrenergic excitation of magnocellular neurons in the rat hypothalamic paraventricular nucleus via intranuclear glutamatergic circuits. *J Neurosci*. 1998; 18:10619–10628. [PubMed: 9852597]
- Dobolyi A, Palkovits M, Bodnar I, Usdin TB. Neurons containing tuberoinfundibular peptide of 39 residues project to limbic, endocrine, auditory and spinal areas in rat. *Neuroscience*. 2003a; 122:1093–1105. [PubMed: 14643775]
- Dobolyi A, Palkovits M, Usdin TB. Expression and distribution of tuberoinfundibular peptide of 39 residues in the rat central nervous system. *J Comp Neurol*. 2003b; 455:547–566. [PubMed: 12508326]
- Dobolyi A, Irwin S, Wang J, Usdin TB. The distribution and neurochemistry of the parathyroid hormone 2 receptor in the rat hypothalamus. *Neurochem Res*. 2006; 31:227–236. [PubMed: 16570212]
- Faber CA, Dobolyi A, Sleeman M, Usdin TB. Distribution of tuberoinfundibular peptide of 39 residues and its receptor, parathyroid hormone 2 receptor, in the mouse brain. *J Comp Neurol*. 2007; 502:563–583. [PubMed: 17394159]
- Fegley DB, Holmes A, Riordan T, Faber CA, Weiss JR, Ma S, Batkai S, Pacher P, Dobolyi A, Murphy A, Sleeman MW, Usdin TB. Increased fear- and stress-related anxiety-like behavior in mice lacking tuberoinfundibular peptide of 39 residues. *Genes Brain Behav*. 2008; 7:933–942. [PubMed: 18700839]
- Ferguson AV, Latchford KJ, Samson WK. The paraventricular nucleus of the hypothalamus—a potential target for integrative treatment of autonomic dysfunction. *Expert Opin Ther Targets*. 2008; 12:717–727. [PubMed: 18479218]
- Fjeldheim AK, Hovring PI, Loseth OP, Johansen PW, Glover JC, Matre V, Olstad OK, Reppe S, Gordeladze JO, Walaas SI, Gautvik KM. Thyrotrophin-releasing hormone receptor 1 and prothyrotrophin-releasing hormone mRNA expression in the central nervous system are regulated by suckling in lactating rats. *Eur J Endocrinol*. 2005; 152:791–803. [PubMed: 15879366]
- Franklin, KBJ.; Paxinos, G., editors. *The mouse brain in stereotaxic coordinates*. 3rd ed. Academic Press; New York: 2008.
- Freneau RT Jr, Troyer MD, Pahner I, Nygaard GO, Tran CH, Reimer RJ, Bellocchio EE, Fortin D, Storm-Mathisen J, Edwards RH. The expression of vesicular glutamate transporters defines two classes of excitatory synapse. *Neuron*. 2001; 31:247–260. [PubMed: 11502256]
- Goldstein J, Perello M, Nillni EA. Preprothyrotrophin-releasing hormone 178–199 affects tyrosine hydroxylase biosynthesis in hypothalamic neurons: a possible role for pituitary prolactin regulation. *J Mol Neurosci*. 2007; 31:69–82. [PubMed: 17416971]
- Herman JP, Prewitt CM, Cullinan WE. Neuronal circuit regulation of the hypothalamo–pituitary–adrenocortical stress axis. *Crit Rev Neurobiol*. 1996; 10:371–394. [PubMed: 8978987]

- Herman JP, Tasker JG, Ziegler DR, Cullinan WE. Local circuit regulation of paraventricular nucleus stress integration: glutamate-GABA connections. *Pharmacol Biochem Behav.* 2002; 71:457–468. [PubMed: 11830180]
- Herman JP, Figueiredo H, Mueller NK, Ulrich-Lai Y, Ostrander MM, Choi DC, Cullinan WE. Central mechanisms of stress integration: hierarchical circuitry controlling hypothalamo–pituitary–adrenocortical responsiveness. *Front Neuroendocrinol.* 2003; 24:151–180. [PubMed: 14596810]
- Hopman AH, Ramaekers FC, Speel EJ. Rapid synthesis of biotin-, digoxigenin-, trinitrophenyl-, and fluorochrome-labeled tyramides and their application for In situ hybridization using CARD amplification. *J Histochem Cytochem.* 1998; 46:771–777. [PubMed: 9603790]
- Hsu DT, Price JL. Paraventricular thalamic nucleus: sub-cortical connections and innervation by serotonin, orexin, and corticotropin-releasing hormone in macaque monkeys. *J Comp Neurol.* 2009; 512:825–848. [PubMed: 19085970]
- Justice NJ, Yuan ZF, Sawchenko PE, Vale W. Type 1 corticotropin-releasing factor receptor expression reported in BAC transgenic mice: implications for reconciling ligand-receptor mismatch in the central corticotropin-releasing factor system. *J Comp Neurol.* 2008; 511:479–496. [PubMed: 18853426]
- Kapoor R, Chapman IM, Willoughby JO. Alpha 2 and beta adrenoceptors in the mediobasal hypothalamus and alpha 2 adrenoceptors in the preoptic-anterior hypothalamus stimulate prolactin secretion in the conscious male rat. *J Neuroendocrinol.* 1993; 5:189–193. [PubMed: 8097944]
- Kawaguchi Y, Shindou T. Noradrenergic excitation and inhibition of GABAergic cell types in rat frontal cortex. *J Neurosci.* 1998; 18:6963–6976. [PubMed: 9712665]
- Kawano H, Daikoku S. Functional topography of the rat hypothalamic dopamine neuron systems: retrograde tracing and immunohistochemical study. *J Comp Neurol.* 1987; 265:242–253. [PubMed: 2891732]
- Kiss JZ, Palkovits M, Zaborszky L, Tribollet E, Szabo D, Makara GB. Quantitative histological studies on the hypothalamic paraventricular nucleus in rats. II. Number of local and certain afferent nerve terminals. *Brain Res.* 1983; 265:11–20. [PubMed: 6850311]
- Lein ES, Hawrylycz MJ, Ao N, Ayres M, Bensinger A, Bernard A, Boe AF, Boguski MS, Brockway KS, Byrnes EJ, Chen L, Chen TM, Chin MC, Chong J, Crook BE, Czaplinska A, Dang CN, Datta S, Dee NR, Desaki AL, Desta T, Diep E, Dolbeare TA, Donelan MJ, Dong HW, Dougherty JG, Duncan BJ, Ebbert AJ, Eichele G, Estin LK, Faber C, Facer BA, Fields R, Fischer SR, Fliss TP, Frensley C, Gates SN, Glattfelder KJ, Halverson KR, Hart MR, Hohmann JG, Howell MP, Jeung DP, Johnson RA, Karr PT, Kawal R, Kidney JM, Knapik RH, Kuan CL, Lake JH, Laramée AR, Larsen KD, Lau C, Lemon TA, Liang AJ, Liu Y, Luong LT, Michaels J, Morgan JJ, Morgan RJ, Mortrud MT, Mosqueda NF, Ng LL, Ng R, Orta GJ, Overly CC, Pak TH, Parry SE, Pathak SD, Pearson OC, Puchalski RB, Riley ZL, Rockett HR, Rowland SA, Royall JJ, Ruiz MJ, Sarno NR, Schaffnit K, Shapovalova NV, Sivisay T, Slaughterbeck CR, Smith SC, Smith KA, Smith BI, Sodt AJ, Stewart NN, Stumpf KR, Sunkin SM, Sutram M, Tam A, Teemer CD, Thaller C, Thompson CL, Varnam LR, Visel A, Whitlock RM, Wornoutka PE, Wolkey CK, Wong VY, Wood M, Yaylaoglu MB, Young RC, Youngstrom BL, Yuan XF, Zhang B, Zwingman TA, Jones AR. Genome-wide atlas of gene expression in the adult mouse brain. *Nature.* 2007; 445:168–176. [PubMed: 17151600]
- Lin W, McKinney K, Liu L, Lakhani S, Jennes L. Distribution of vesicular glutamate transporter-2 messenger ribonucleic Acid and protein in the septum-hypothalamus of the rat. *Endocrinology.* 2003; 144:662–670. [PubMed: 12538629]
- Liposits Z. Ultrastructure of hypothalamic paraventricular neurons. *Crit Rev Neurobiol.* 1993; 7:89–162. [PubMed: 8102325]
- Liu P, Jenkins NA, Copeland NG. A highly efficient recombineering-based method for generating conditional knockout mutations. *Genome Res.* 2003; 13:476–484. [PubMed: 12618378]
- Meites J. Neuroendocrine control of prolactin in experimental animals. *Clin Endocrinol.* 1977; 6(Suppl):9S–18S.
- Merchenthaler I, Lennard DE. The hypophysiotropic neurotensin-immunoreactive neuronal system of the rat brain. *Endocrinology.* 1991; 129:2875–2880. [PubMed: 1954874]

- Mezey E, Kiss JZ. Vasoactive intestinal peptide-containing neurons in the paraventricular nucleus may participate in regulating prolactin secretion. *Proc Natl Acad Sci USA*. 1985; 82:245–247. [PubMed: 3881755]
- Moga MM, Weis RP, Moore RY. Efferent projections of the paraventricular thalamic nucleus in the rat. *J Comp Neurol*. 1995; 359:221–238. [PubMed: 7499526]
- Myers RD. Injection of solutions into cerebral tissue: relation between volume and diffusion. *Physiology and Behavior*. 1966; 1:171–174.
- Nagy GM, Bodnar I, Banky Z, Halasz B. Control of prolactin secretion by excitatory amino acids. *Endocrine*. 2005; 28:303–308. [PubMed: 16388120]
- Nillni EA, Sevarino KA, Jackson IM. Identification of the thyrotropin-releasing hormone-prohormone and its post-translational processing in a transfected AtT20 tumoral cell line. *Endocrinology*. 1993; 132:1260–1270. [PubMed: 8440187]
- O’Gorman S, Dagenais NA, Qian M, Marchuk Y. Protamine-Cre recombinase transgenes efficiently recombine target sequences in the male germ line of mice, but not in embryonic stem cells. *Proc Natl Acad Sci USA*. 1997; 94:14602–14607. [PubMed: 9405659]
- Palkovits M, Baffi JS, Pacak K. The role of ascending neuronal pathways in stress-induced release of noradrenaline in the hypothalamic paraventricular nucleus of rats. *J Neuroendocrinol*. 1999; 11:529–539. [PubMed: 10444310]
- Pohl CR, Lee LR, Smith MS. Qualitative changes in luteinizing hormone and prolactin responses to N-methyl-aspartic acid during lactation in the rat. *Endocrinology*. 1989; 124:1905–1911. [PubMed: 2647467]
- Rasband, WS. Image J. Bethesda, MD: U.S. National Institutes of Health; 1997–2009.
- Rittenhouse PA, Levy AD, Li Q, Bethea CL, Van de Kar LD. Neurons in the hypothalamic paraventricular nucleus mediate the serotonergic stimulation of prolactin secretion via 5-HT_{1c/2} receptors. *Endocrinology*. 1993; 133:661–667. [PubMed: 8344205]
- Roland BL, Sawchenko PE. Local origins of some GABAergic projections to the paraventricular and supraoptic nuclei of the hypothalamus in the rat. *J Comp Neurol*. 1993; 332:123–143. [PubMed: 7685780]
- Sawchenko PE. Adrenalectomy-induced enhancement of CRF and vasopressin immunoreactivity in parvocellular neurosecretory neurons: anatomic, peptide, and steroid specificity. *J Neurosci*. 1987a; 7:1093–1106. [PubMed: 3553442]
- Sawchenko PE. Evidence for differential regulation of corticotropin-releasing factor and vasopressin immunoreactivities in parvocellular neurosecretory and autonomic-related projections of the paraventricular nucleus. *Brain Res*. 1987b; 437:253–263. [PubMed: 3325130]
- Sawchenko PE, Swanson LW. The organization of noradrenergic pathways from the brainstem to the paraventricular and supraoptic nuclei in the rat. *Brain Res*. 1982; 257:275–325. [PubMed: 6756545]
- Sawchenko PE, Swanson LW. Localization, colocalization, and plasticity of corticotropin-releasing factor immunoreactivity in rat brain. *Fed Proc*. 1985; 44:221–227. [PubMed: 2981743]
- Sawchenko PE, Swanson LW, Grzanna R, Howe PR, Bloom SR, Polak JM. Colocalization of neuropeptide Y immuno-reactivity in brainstem catecholaminergic neurons that project to the paraventricular nucleus of the hypothalamus. *J Comp Neurol*. 1985; 241:138–153. [PubMed: 3840810]
- Semenenko FM, Cuello AC, Goldstein M, Lee KY, Sidebottom E. A monoclonal antibody against tyrosine hydroxylase: application in light and electron microscopy. *J Histochem Cytochem*. 1986; 34:817–821. [PubMed: 2871071]
- Smith DW, Day TA. c-fos Expression in hypothalamic neurosecretory and brainstem catecholamine cells following noxious somatic stimuli. *Neuroscience*. 1994; 58:765–775. [PubMed: 8190253]
- Sugimura Y, Murase T, Ishizaki S, Tachikawa K, Arima H, Miura Y, Usdin TB, Oiso Y. Centrally administered tuberoinfundibular peptide of 39 residues inhibits arginine vasopressin release in conscious rats. *Endocrinology*. 2003; 144:2791–2796. [PubMed: 12810532]
- Swanson LW, Sawchenko PE. Hypothalamic integration: organization of the paraventricular and supraoptic nuclei. *Annu Rev Neurosci*. 1983; 6:269–324. [PubMed: 6132586]

- Toth ZE, Mezey E. Simultaneous visualization of multiple antigens with tyramide signal amplification using antibodies from the same species. *J Histochem Cytochem*. 2007; 55:545–554. [PubMed: 17242468]
- Usdin TB. The PTH2 receptor and TIP39: a new peptide-receptor system. *Trends Pharmacol Sci*. 2000; 21:128–130. [PubMed: 10740285]
- Usdin TB, Hoare SR, Wang T, Mezey E, Kowalak JA. TIP39: a new neuropeptide and PTH2-receptor agonist from hypothalamus. *Nat Neurosci*. 1999; 2:941–943. [PubMed: 10526330]
- Usdin TB, Paciga M, Riordan T, Kuo J, Parmelee A, Petukova G, Camerini-Otero RD, Mezey E. Tuberoinfundibular peptide of 39 residues is required for germ cell development. *Endocrinology*. 2008; 149:4292–4300. [PubMed: 18483145]
- Vale W, Vaughan J, Yamamoto G, Bruhn T, Douglas C, Dalton D, Rivier C, Rivier J. Assay of corticotropin releasing factor. *Methods Enzymol*. 1983; 103:565–577. [PubMed: 6321896]
- Van de Kar LD, Blair ML. Forebrain pathways mediating stress-induced hormone secretion. *Front Neuroendocrinol*. 1999; 20:1–48. [PubMed: 9882535]
- van den Pol AN, Trombley PQ. Glutamate neurons in hypothalamus regulate excitatory transmission. *J Neurosci*. 1993; 13:2829–2836. [PubMed: 8101211]
- van den Pol AN, Wuarin JP, Dudek FE. Glutamate, the dominant excitatory transmitter in neuroendocrine regulation. *Science*. 1990; 250:1276–1278. [PubMed: 1978759]
- Van der Krans A. Labeling of neurons following intravenous injections of fluorescent tracers in mice. *J Neurosci Methods*. 1983; 9:95–103. [PubMed: 6645606]
- Varoqui H, Schafer MK, Zhu H, Weihe E, Erickson JD. Identification of the differentiation-associated Na⁺/PI transporter as a novel vesicular glutamate transporter expressed in a distinct set of glutamatergic synapses. *J Neurosci*. 2002; 22:142–155. [PubMed: 11756497]
- Wang J, Palkovits M, Usdin TB, Dobolyi A. Afferent connections of the subparafascicular area in rat. *Neuroscience*. 2006a; 138:197–220. [PubMed: 16361065]
- Wang J, Palkovits M, Usdin TB, Dobolyi A. Forebrain projections of tuberoinfundibular peptide of 39 residues (TIP39)-containing subparafascicular neurons. *Neuroscience*. 2006b; 138:1245–1263. [PubMed: 16458435]
- Wang T, Palkovits M, Rusnak M, Mezey E, Usdin TB. Distribution of parathyroid hormone-2 receptor-like immunoreactivity and messenger RNA in the rat nervous system. *Neuroscience*. 2000; 100:629–649. [PubMed: 11098126]
- Ward HL, Small CJ, Murphy KG, Kennedy AR, Ghatei MA, Bloom SR. The actions of tuberoinfundibular peptide on the hypothalamo-pituitary axes. *Endocrinology*. 2001; 142:3451–3456. [PubMed: 11459790]
- Wittmann G, Lechan RM, Liposits Z, Fekete C. Glutamatergic innervation of corticotropin-releasing hormone- and thyrotropin-releasing hormone-synthesizing neurons in the hypothalamic paraventricular nucleus of the rat. *Brain Res*. 2005; 1039:53–62. [PubMed: 15781046]
- Wu P, Jackson IM. Post-translational processing of thyrotropin-releasing hormone precursor in rat brain: identification of 3 novel peptides derived from proTRH. *Brain Res*. 1988; 456:22–28. [PubMed: 3136859]
- Xu X, Roby KD, Callaway EM. Mouse cortical inhibitory neuron type that coexpresses somatostatin and calretinin. *J Comp Neurol*. 2006; 499:144–160. [PubMed: 16958092]
- Zhang BJ, Kusano K, Zervas P, Iacangelo A, Young WS 3rd, Gainer H. Targeting of green fluorescent protein to secretory granules in oxytocin magnocellular neurons and its secretion from neurohypophysial nerve terminals in transgenic mice. *Endocrinology*. 2002; 143:1036–1046. [PubMed: 11861530]
- Ziegler DR, Herman JP. Local integration of glutamate signaling in the hypothalamic paraventricular region: regulation of glucocorticoid stress responses. *Endocrinology*. 2000; 141:4801–4804. [PubMed: 11108297]
- Ziegler DR, Cullinan WE, Herman JP. Distribution of vesicular glutamate transporter mRNA in rat hypothalamus. *J Comp Neurol*. 2002; 448:217–229. [PubMed: 12115705]

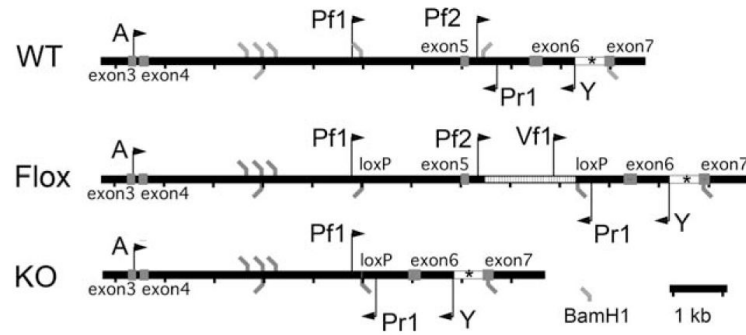


Figure 1.

Generation and genotyping of PTH2R knockout mice. A 10-kb PTH2R fragment extending from A to Y was used for recombination. ES clones with homologous recombination were identified by Southern blot using BamH1 digestion and the indicated probe sequence (asterisk). PCR of genomic DNA using primers Pf2 and Pr1 produced a 635-bp band from a wild-type (WT) allele, primers Vf1 and Pr1 produced a 775-bp band from the floxed-exon-5 (Flox) allele, and primers Pf1 and Pr1 produced a 507-bp band from the exon-5-deleted (KO) allele.

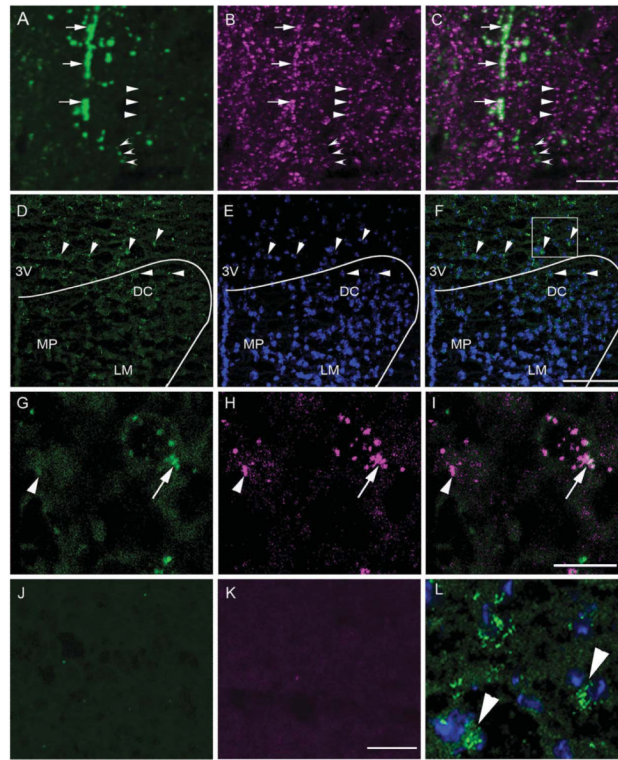


Figure 2.

Coexpression between PTH2R and VGlut2 immunoreactivity and PTH2R and VGlut2 mRNA in the PVN area. High-magnification confocal images show PTH2R-ir fibers (**A**; green), VGlut2-ir fibers (**B**; magenta), and a merged image (**C**). Open arrowheads point to a fiber with only PTH2R-ir, solid arrowheads to a fiber with only VGlut2-ir, and arrows to PTH2R-ir/VGlut2-ir fibers. **D**: Distribution of PTH2R mRNA in the dorsal part of the PVN and adjacent peri-PVN area as detected by fluorescent in situ hybridization. The arrowheads point to cells expressing PTH2R mRNA (green). **E** shows DAPI counterstaining (blue), which aids visualization of the anatomical distribution of the mRNA signal. **F** is a merged image of the PTH2R mRNA signal and the DAPI counterstain. The curved line indicates the approximate position of the PVN. High-magnification confocal images in the third row show expression of VGlut2 mRNA (**G**; green), PTH2R mRNA (**H**; magenta), and a merged image (**I**). Arrow points to a double-labeled cell and an arrowhead to a cell containing only PTH2R signal. Controls with riboprobes omitted show specificity of the immunodetection of VGlut2 (**J**) and PTH2R (**K**) haptens. **L**: Enlarged image of the boxed area in **F**. 3V, Third ventricle; DC, paraventricular dorsal cap parvocellular cell group; LM, paraventricular lateral magnocellular cell group; MP, paraventricular medial parvocellular cell group. Scale bars 10 μm in **C** (applies to **A**–**C**); 10 μm in **I** (applies to **G**–**I**); 10 μm in **K** (applies to **J**–**L**); 100 μm in **F** (applies to **D**–**F**). [Color figure can be viewed in the online issue, which is available at wileyonlinelibrary.com.]

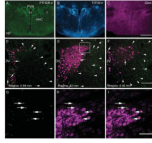


Figure 3.

PTH2R, TIP39, and glutamate immunoreactivity in the hypothalamic paraventricular nucleus (PVN) and the adjacent region of the anterior hypothalamus. Dense networks of PTH2R-ir (**A**; green), TIP39-ir (**B**; cyan), and glutamate-ir (**C**; magenta) fibers are present in the PVN as well as in the adjacent peri-PVN zone, as shown at -0.94 mm to bregma (Franklin and Paxinos, 2008). **A–C** are widefield images. **D–F** are confocal images of β -gal-ir distribution in the PVN area at the indicated levels from a PTH2R lacZ knock-in mouse. Fluorogold (FG-ir)-labeled neuroendocrine neurons that define the neuroendocrine part of PVN are shown in magenta. β -Gal-ir is contained in minute precipitates (green specks). Examples within the PVN are indicated with arrows and in the adjacent area with arrowheads. **G–I**: Higher magnification images from the boxed PVN region in **E** show β -gal-ir (**G**), FG-ir (**H**), and a merged image (**I**), with little apparent coexpression between FG-ir and β -gal-ir. 3V, Third ventricle; AHC, anterior hypothalamic area, central; f, fornix; LH, lateral hypothalamus; opt, optic tract; PVN, paraventricular nucleus. Scale bars = $200 \mu\text{m}$ in **C** (applies to **A–C**); $100 \mu\text{m}$ in **F** (applies to **D–F**); $50 \mu\text{m}$ in **I** (applies to **G–I**). [Color figure can be viewed in the online issue, which is available at wileyonlinelibrary.com.]

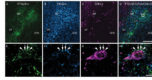
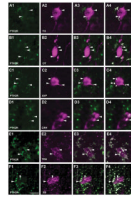
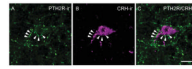


Figure 4.

Relationship among PTH2R-ir, TIP39-ir, and CRH-ir in the PVN. Images show PTH2R-ir (A; green), TIP39-ir (B; cyan), and CRH-ir (C; magenta) in the PVN. E (PTH2R-ir), F (TIP39-ir), G (CRH-ir), and H (PTH2R/TIP39/CRH-ir) are high-magnification images of the boxed area in D. Arrowheads point to PTH2R-ir, and arrows point to TIP39-ir labeled fibers adjacent to the same CRH-ir neuron (magenta). Images in E–H are 3D renderings created using the command “3D opacity” in Volocity 64 from a Z series of 12 0.5- μ m sections covering 6 μ m in the Z-axis. AHA, anterior hypothalamic area; MP, paraventricular medial parvocellular cell group; VP, paraventricular ventral parvocellular cell group. Scale bars = 100 μ m in D (applies to A–D); 10 μ m in H (applies to E–H). [Color figure can be viewed in the online issue, which is available at wileyonlinelibrary.com.]

**Figure 5.**

Relationship between PTH2R and neuroendocrine immunoreactivity in the PVN area. PTH2R-ir fibers are green in all images. Magenta labels tyrosine hydroxylase (TH; **A2–4**), oxytocin (OT; **B2–4**), arginine-vasopressin (AVP; **C2–4**), corticotrophin-releasing hormone (CRH; **D2–4**), thyrotropin-releasing hormone (TRH; **E1–4**), and somatostatin (SS; **F2–4**). Single channels are shown in the first and second columns, merged images in the third column, and merged images in which regions containing suprathreshold levels of both labels are pseudocolored white are in the fourth column. Arrowheads and the white pseudocolor in the fourth column indicate touching points, as defined by areas that contain both green and magenta labeling above threshold. Images are single optical sections; analysis was performed on Z-series as described in Materials and Methods. Scale bar = 10 μm . [Color figure can be viewed in the online issue, which is available at wileyonlinelibrary.com.]

**Figure 6.**

High-magnification image of PTH2R-ir fibers (**A**; green) and a CRH-ir cell (**B**; magenta) in the PVN. **C** shows PTH2R/CRH merged image of a CRH-ir neuron enveloped by PTH2R-ir fibers, indicated by arrowheads. The image is a 3D rendering created using the command “3D opacity” in Volocity 64 from a Z-series of 12 0.5- μm sections covering 6 μm in the Z-axis. Scale bar = 10 μm . [Color figure can be viewed in the online issue, which is available at wileyonlinelibrary.com.]

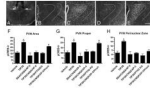


Figure 7.

Expression of pCREB-ir after TIP39 infusion into the PVN. **A:** Typical cannula positions are indicated by arrows. **B–E:** Expression of pCREB-ir 15 minutes following test agent administration. **B:** Note very low expression after the infusion of vehicle. **C:** p-CREB-ir is present in the PVN and peri-PVN area following 100 pmol TIP39. **D:** Expression of p-CREB-ir is much less after the infusion of 100 pmol TIP39 plus 30 pmol each of CNQX and AP-5. **E:** p-CREB-ir is obvious in the PVN proper after the infusion of 100 pmol TIP39 plus CNQX/AP-5 (30 pmol each) followed by a hind paw pinch. DAPI counterstaining (not shown) was used to draw the curved lines that outline the peri-PVN zone where pCREB-ir was counted in addition to the PVN proper. Graphs show counts of the PVN neurons expressing pCREB-ir following administration of TIP39 with or without glutamate receptor blockers. **F:** PVN area (PVN nucleus plus peri-PVN zone). **G:** PVN nucleus proper. **H:** Peri-PVN zone. Significantly different from vehicle-treated animals, $*P < 0.0001$, $\#P < 0.001$; ANOVA followed by Student-Neuman-Keuls test, $n = 4–6$ /group. Scale bar = 100 μm .

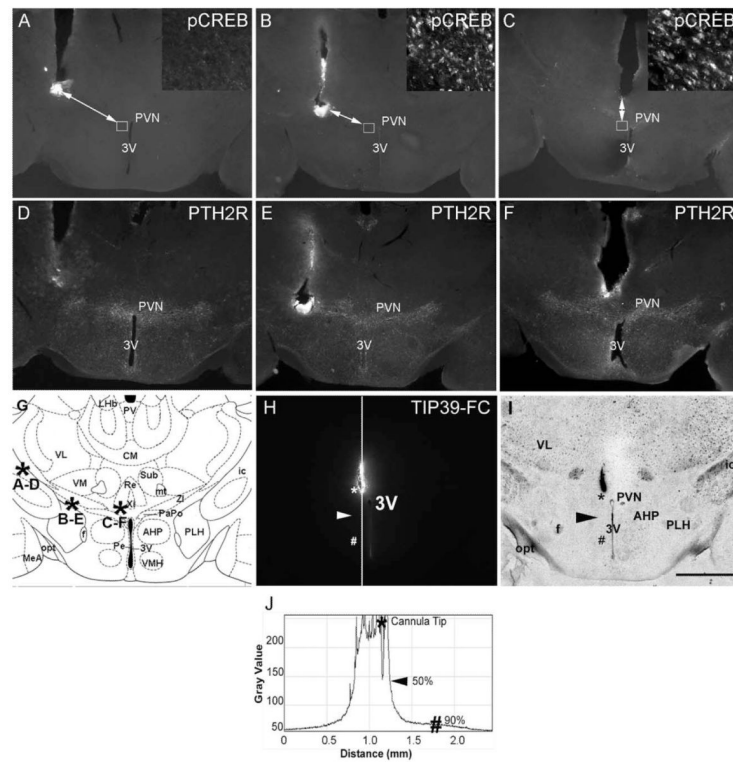


Figure 8.

Evaluation of TIP39 diffusion and dependence of p-CREB-ir expression in the PVN on injector placement. **A–C** show p-CREB immunolabeling. **D–F** show PTH2R immunolabeling of sections adjacent to the upper row sections. **A** and **D** show injector placement outside the PVN area expressing PTH2R-ir. **B** and **E** show injector placement at the border of the PVN area expressing PTH2R-ir. **C** and **F** show injector placement into the medial part of the PVN area expressing PTH2R-ir. Insets in **A–C** are high-magnification images of p-CREB-ir taken from the areas outlined by the small squares. The arrows in **A–C** connect the end point of injector tracks to the areas of p-CREB-ir expression shown in the inserts and are markers for the effective distance of TIP39 spread 15 minutes after infusion of 0.5 μ l. **G** is a matched atlas plate (Franklin and Paxinos, 2008) of the brain area shown in the first six panels. Asterisks indicate the placement of injector tips with the corresponding panels indicated by letters. **H** shows the area covered by fluorescent labeled TIP39 (TIP39-FC) 15 minutes after the infusion of 0.5 μ l into the PVN, as determined by plotting the gray value against the distance. The asterisks mark the injector tip and the peak intensity value. The arrowhead indicates a point of 50% decrease in signal intensity, and the number symbol indicates a point of 90% decrease in signal. **I** is a brightfield image of the field shown in **H** with visible anatomical landmarks. **J** plots gray value vs. distance along the white line in **H**, used to estimate TIP39 diffusion. 3V, Third ventricle; AHP, anterior hypothalamic area, posterior; CM, central medial thalamic nucleus; f, fornix; ic, internal capsule; mt, mammillothalamic tract; MeA, medial amygdala; opt, optic tract; PaPo, paraventricular hypothalamic nucleus, posterior; Pe, periventricular hypothalamic nucleus; PLH, peduncular part of the lateral hypothalamus; Re, reuniens thalamic nucleus; Sub, submedius thalamic nucleus; VM, ventromedial thalamic nucleus; VMH, ventromedial hypothalamic nucleus; VL, ventrolateral thalamic nucleus; ZI, zona incerta. Scale bar = 0.5 mm.

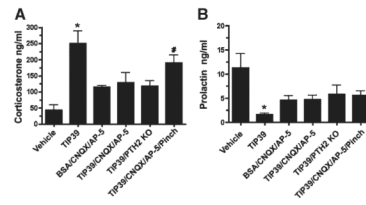


Figure 9.

Plasma hormone levels following administration of TIP39 with or without glutamate receptor blockers. **A:** Plasma corticosterone. **B:** Plasma prolactin. Treatment groups as defined in the legend to Figure 8. Significantly different from vehicle-treated animals, * $P < 0.0006$, # $P < 0.01$; ANOVA followed by Student-Neuman-Keuls test, $n = 4-7$ /group.

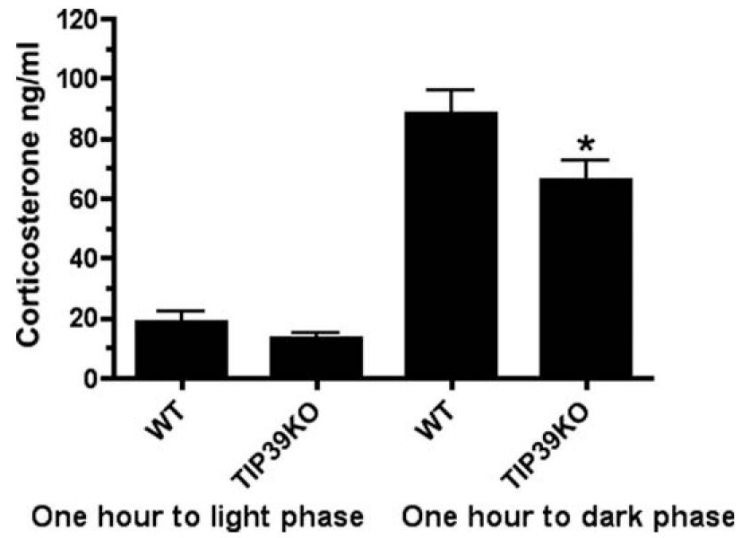


Figure 10. Plasma corticosterone levels in wild-type (WT) and TIP39 knockout (KO) mice 1 hour before the light phase and 1 hour before the dark phase of the day. Significantly different from wild-type mice at the same time point, * $P < 0.01$; ANOVA followed by Student-Neuman-Keuls test, $n = 8-13$ /group.

TABLE 1

Antibodies Used for Immunohistochemistry

Antigen	Immunogen	Source	Dilution
Arginine-vasopressin specific neurophysin	Rat posterior pituitary extract, keyhole limpet hemocyanin (KLH) coupled	Dr. Harold Gainer, NIH; mouse monoclonal PS41	1:1,000
β -Galactosidase	Purified full-length native protein	AbCann, Cambridge, MA; chicken No. AB9361	1:15,000
Corticotrophin releasing-hormone	Synthetic peptide corresponding to full-length rat/human CRF(1-41)	Dr. Wylie Vale, Salk Institute; rabbit polyclonal PBL rC70 pool 397-223	1:5,000
Fluorogold	Fluorogold (hydroxystilbamidine)	Chemicon; rabbit polyclonal AB153	1:1,000
Glutamate	Glutamate-glutaraldehyde conjugate	Chemicon; rabbit polyclonal AB5018C	1:1,000
Oxytocin-specific neurophysin	Rat posterior pituitary extract, KLH coupled	Dr. Harold Gainer, NIH; mouse monoclonal PS38	1:1,000
pCREB	Synthetic phosphopeptide CSRRP _s YRKL, where s represents phospho-Ser133 of human CREB, coupled to KLH	Cell Signaling, Danvers, MA; rabbit monoclonal catalog 9198L	1:1,000
PTH2-R	Synthetic peptide corresponding to residues 480-500 of the rat PTH2R (GenBank U55836), KLH coupled	Dr. T. Usdin, NIH; rabbit polyclonal 2710	1:20,000, 1:5,000
Somatostatin	Synthetic 1-14 cyclic somatostatin, thyroglobulin coupled	Chemicon; rat monoclonal catalog MAB354	1:1,000
Thyrotropin releasing-hormone	Prepro-TRH ₂₄₀₋₂₅₅ , bovine thyroglobulin coupled	Dr. Eduardo Nillni, Brown University; rabbit polyclonal pYE17	1:1,000
TIP39	Full-length TIP39, KLH coupled	Dr. T. Usdin, NIH; rabbit polyclonal pooled 7250, 7251	1:3,000
Tyrosine hydroxylase	Tyrosine hydroxylase purified from PC12 cells	Chemicon; mouse monoclonal catalog MAB358	1:1,000
VGlut2	GST fusion protein containing AA 519-582 of rat VGlut2	Dr. Robert Edwards, UCSF; rabbit polyclonal	1:10,000